

## ULTRASONIC TRANSDUCERS, IMAGING

Modern ultrasound imaging systems, as exemplified by those systems used in medical diagnosis, are critically dependent upon electroacoustic transducers and the associated front-end electronics for the generation of insonifying pulses, the detection of reflected echoes, and the conversion of data to digital form (1). Major characteristics of these ultrasonic imaging systems are determined by the electro-acoustic transducer alone. Its fundamental resonance sets the center frequency, which ranges from 2 MHz to 12 MHz for general imaging to 40 MHz for the skin and eye. The transducer damping sets the bandwidth and thus the attainable range resolution (in

pulse-echo operation), and its diffraction focusing the attainable lateral resolution. Although many different designs are used in ultrasonic and acoustic imaging in marine and industrial applications, the most advanced types are found in medical diagnostic imaging, and these will be described here.

The active elements of a transducer are mounted within a probe or scan head that contains any elements needed for mechanical scanning, acoustic damping and focusing structures, and electrical connections. Representative types are shown in Fig. 1. In some designs all or part of the electronics for transmit and receive beamforming are also mounted in the probe. These purely electronic circuits play an important role in determining the performance of multielement arrays. For example, these circuits use timing delays and switching to control the direction and focusing of the transmitted beam. During the receive interval similar delays are introduced to scan and focus the region of maximum sensitivity, called the receiving beam.

The sound beam emitted by a single-element round transducer is shown in Fig. 2. This beam is formed by diffraction of the nearly plane waves being emitted from a large diameter area compared to the wavelength. The field shown is for a continuous wave, which forms many peaks and nulls in the near field because of wave interference. For typical pulse operation these nulls occur at different places for each frequency in the pulse, so the pattern is blurred, with filling of the nulls and lowering of the peaks. Both transmitted and receiving beams for this transducer would have the same shape.

The basic transducer shown in cross-section in Fig. 3(a), consists of a vibrating element (usually a ceramic material but often called a crystal) that is one-half wavelength thick at the nominal resonant frequency. Currently, transducers are made from either conventional solid piezoelectric ceramics such as lead zirconate-titanate (PZT) or their composites, which are part ceramic and part plastic (2).

The ceramic or composite crystal is mounted, as shown in Fig. 3(a), in a sandwich with materials selected to damp the



**Figure 1.** Representative types of medical imaging transducers. From left: a mechanically scanned and a strongly curved linear array endoscopes, a curved linear array, a linear phased array, and a side-looking linear array for imaging during surgery. (Courtesy of Siemens Medical Systems, Inc. Ultrasound Group)

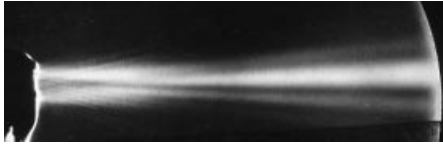


**Figure 2.** Cross-section of the continuous wave acoustic field, shown in white, from a single element transducer visualized in water by the Schlieren technique. Note the far field to the right where the beam has a major lobe flanked by sidelobes. Closer to the transducer is the near field where interference effects dominate, producing zeros and maxima of pressure amplitude.

vibrations and to focus the radiated acoustic energy. The structures are commonly cemented together by epoxy resins. This layered construction is used for single-element transducers as well as for the individual elements of arrays, described next.

The scanning acoustic microscope (3) uses a construction similar to that shown in Fig. 3(a), but uses zinc oxide piezoelectric films on a strongly focused sapphire lens for operation in the microwave region. Two such strongly focused transducers are used facing each other with a common focal point (confocal arrangement) and mechanically scanned over a sample immersed in water or oil for transmission measurements. A single such transducer can be operated in pulse echo mode, and these are useful for investigating the subsurface layers in integrated circuits. Another form of microscope operates at lower frequencies to penetrate samples and uses a laser beam for readout of the transmitted waves in real time (4).

The most versatile imaging systems use array transducers which have many (32 to 512) small elements that are less than the acoustic wavelength in the propagating medium wide; see Fig. 4. The functions of scanning and focusing are performed by electronic rather than mechanical means by switching and delaying the electrical signals to and from the elements, just as in antenna arrays. A major difference is that in ultrasonic imaging the patient can be within the near field region where strong focusing is effective. With dynamic focusing the focal region can be moved during the pulse receive

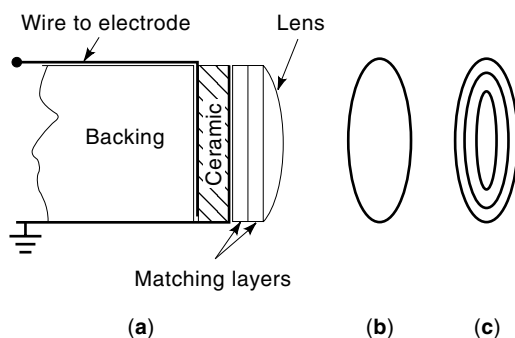


**Figure 3.** Cross section of a single transducer element at (a), showing the vibrating crystal with backing material to damp the vibrations and two approximately quarter-wave impedance matching layers on the radiating face. The curvature of the lens shown is for a rubber material with speed of sound less than that of water. Solid lenses with a higher sound speed are concave on the face. The crystal of a single element transducer can be solid as at (b), or subdivided into a series of annuli as at (c).

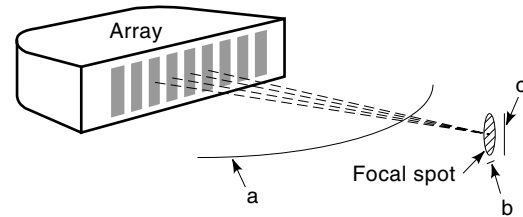


**Figure 4.** Geometry of the field from a linear or phased array transducer, showing how several elements scan a sound beam over a plane, (a). The focal spot is small in the image plane for the best resolution, (b). In the out-of-plane or elevation direction, the resolution element, (c) is larger since the focusing is weaker. This dimension is also called the slice, or transverse, thickness.

interval to track the position of the origin of the received pulse, so the receiver is focused at all depths without regard for depth of field.

## TYPES OF TRANSDUCERS

Single-element transducers are used in mechanical scanners, mainly at high ultrasonic frequencies where arrays that require small elements are expensive or impossible to construct with current technologies, or where a wide scanned field is required for an inexpensive system design. The smallest transducers of all, less than one mm in diameter, are used to scan inside blood vessels. The transducer is side-looking and mechanically rotated to scan.

The basic linear array is shown in Fig. 4, and the different scan formats from arrays in Fig. 5. The details of scanning operations are set by timing the electrical excitation to the transducer elements, and using time delays on receive for focusing. True time delays must be used because of the wide bandwidth needed for short pulses. This is in contrast to the phase shifts used in radar. The most simple method of scanning is to select a subset of elements for each beam, and then translate this group across the array to scan, producing a rectilinear image. The width of the scanned field is set by the length of the array. An expanding aperture is used to keep the lateral resolution nearly constant with depth. That is, the number of elements in the scanned group is increased with time after the pulse is transmitted.

Phased linear arrays are scanned by selecting timing and delays to swing the beam across the scan plane to produce a

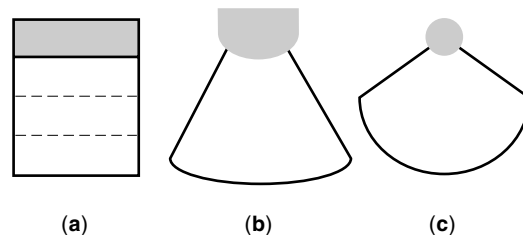


**Figure 5.** Scan plane and image formats from (a) a rectilinear array, (b) a curvilinear array, and at (c) a sector scan. Sector scans are formed by mechanical scanners and phased linear arrays. The field in (a) is subdivided to show the focal regions on transmit. For the best resolution the beam is focused in these regions sequentially and the image constructed from the three scans.

**Table 1. Approximate Values of Some Properties of Ceramics Used in Imaging Transducers**

Material	$Z_0$	$v$	$k_t$	$\epsilon_r$	$h$
PZT 5	34	4400	0.49	830	$22 \times 10^8$
PZT 5 h	32	4100	0.52	1700	$18 \times 10^8$
PZT 5 composite 80 to 20% PZT	25–8	3900–3500	0.65	700–200	$(22 \text{ to } 17) \times 10^8$

sector scan, as shown in Fig. 5(c). In the most advanced arrays the functions of scanning, dynamic focusing, expanding aperture, and lateral translation may be combined. The phased array will have a surface area that is smaller than the image field. They are commonly used for imaging the heart through the window between the ribs.

Curvilinear arrays are an economical solution for many low end applications since they avoid the need for phasing to scan the beam. A flexible composite ceramic element and the attached layers are curved in an arc so that simple linear translation of the excitation results in a sector scan with a suppressed center; see Fig. 5(b).

The annular array system uses a ceramic that is circular with the radiating areas divided into concentric annuli; see Fig. 3(c). The electrical connections are made to each ring electrode. It uses electronic transmit and dynamic receive focusing combined with mechanical motions for scanning. The resolution is equal in both azimuth and elevation directions to reduce unwanted and confusing signals from structures near, but not in, the image plane.

Linear arrays are also classified as 1-D, 2-D, or something in-between, although they are actually two-dimensional structures. A 1-D array has a number of elements arranged in a line as shown in Fig. 4. Weak focusing is applied to the long (elevation) dimension of the elements to reduce the thickness of the beam in the scanned plane. A cylindrical lens is molded onto the radiating face, as in the linear arrays shown in Fig. 1.

Arrays can be made very small. A catheter mounted array for imaging inside blood vessels (20 MHz, 64 elements) is currently 3 mm in diameter, and other arrays can be as small as a centimeter for pediatric transesophageal scanning up to several centimeters for general extracorporeal use.

A full 2-D array is divided into nearly equal numbers of elements in two directions, and the beam can be controlled to scan in three dimensions with equal resolution in azimuth and elevation. To have resolution equivalent to linear arrays these 2-D structures must have enormous numbers of elements, and these present many construction and electrical problems that are only now being solved. For example, to compete with a 128 element array the 2-D structure would need 16,384 elements.

## BASIC CONSTRUCTION

### Materials

The crystal materials are commonly ceramics based on lead zirconate titanates (PZT), which are electrostrictive materials (2). The major faces of half-wave thick ceramic plates are plated with metal electrodes for electrical connections. They are made piezoelectric by applying a high electric field on the

order of 20 kV/cm to the electrodes while the material is held above its Curie temperature to align the molecular domains, called a *poling process*. The materials are then cooled below this point with the field in place, after which they exhibit the property of piezoelectricity and can transduce signals linearly between electrical and mechanical energy.

Approximate properties of ceramics are shown in Table 1.  $Z_0$  is the characteristic acoustic impedance in MRayls;  $v$ , the speed of compressional waves (m/s);  $k_t$  the planar coupling coefficient;  $\epsilon_r$  the relative dielectric constant and  $h$  the piezoelectric coefficient, (V/m). Table 1 was compiled from various sources; manufacturers' data, preferably measured on a specific lot of material, should be followed for commercial design.

The center frequency is set by using ceramic plates that have been ground to half-wave thickness (measured at the speed of sound in the ceramic or composite material). The resonance frequency usually shifts downward from the nominal value when the element is loaded by other materials and tissue due to the electromechanical coupling. The rate of energy transfer into a load for a ceramic element of many wavelengths diameter is described by the thickness coupling coefficient, see Table 1. (Note that some tabulated values of  $k$  are called  $k_{\text{eff}}$ ; this is the square of the coupling coefficient.) The coupling coefficient for large area ceramics is  $k_t$ , while the higher value,  $k_{33}$ , is approached for very narrow elements and the pillars of composite materials.

The solid ceramic materials have a plane wave characteristic acoustic impedance of about 30 MRayls, much higher than tissue of 1.5 MRayls. (1 Rayl = density times sound speed.) Therefore energy leaves them over many cycles, lengthening the pulse. Composite materials have a better impedance match (5). To produce a composite material ceramics are diced with many fine saw cuts, as in Fig. 6, and the grooves (kerfs) are filled with a soft polymer. This composite ceramic has a lower acoustic impedance for higher damping and a higher coupling coefficient, approaching  $k_{33}$ . In this way the overall

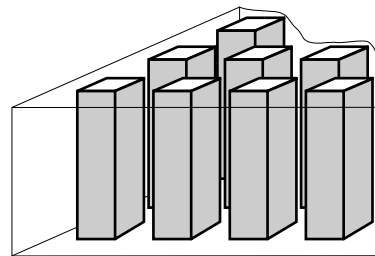


**Figure 6.** Structure of a composite ceramic with ceramic pillars surrounded by an inactive polymer. The solid ceramic material is typically diced in two directions half-way through its thickness. The space is filled with polymer, the material turned over, and matching saw cuts made from the other side, which are then filled.

electromechanical conversion rate can be maximized to exceed that of solid PZT material.

These composites vibrate as a homogenous material as long as the lateral dimensions of the ceramic pillars and polymer fillings are much less than the wavelength. Composites are restricted to the lower frequency range since saws capable of making kerf widths less than the 15  $\mu\text{m}$  currently available are needed to extend composite technology into higher frequencies. The design of these composite materials is complicated by the need for proper design to suppress waves that travel in the lateral direction through the periodic structure presented by the dicing (6). See the section "Finite Element Models" in this article for further details.

### Assembly

Because the acoustic impedance of solid or composite ceramics is still high compared to water or tissue the resonant crystals have a narrow bandwidth unless acoustical damping and matching materials are applied. Composites are a better impedance match, but additional steps are still needed to allow operation over the very wide bandwidths currently in use. The radiating face produces useful output so it is usually matched with several thin layers of material designed as a transmission line transformer, see Fig. 3(a). Desilets has published the analytic design of these approximately quarter-wave structures (7).

The structures on the radiating face can also provide insulation for electrical safety and shielding for reduction of electromagnetic interference and for acoustic focusing. Further damping is provided if needed by backing materials which widen the bandwidth at the expense of efficiency. These matching materials are rubbers or plastics loaded with inorganic powders to raise their impedance to values intermediate between ceramics and tissue. Additional additives provide for increased losses in the backing and for easy casting.

In modern designs using composites the transducer bandwidth can be greater than needed for operation with a pulse having a single center frequency. The extra bandwidth is used to allow changing the center frequency while scanning, or to provide for frequency interlacing of a second sound beam used for Doppler flow detection.

The acoustic field, see Fig. 2, has two regions. The *near field* or Fresnel region in which the differences of the path lengths from any point on the radiating face of the transducer to any field point are larger than a half-wavelength exhibits interference effects. At greater ranges a far field or Fraunhofer region exists, where the interference effects do not appear except off the axis of the main lobe of the beam. The field can be focused in the near field region by forming a lens shaped like a section of a sphere or cylinder, or by forming the crystal into this shape by grinding before polarizing.

In the far field the main sound beam diverges with an angle  $\Theta$ , given by:

$$\sin \Theta \approx \lambda/D \quad (1)$$

where  $\lambda$  is the acoustic wavelength and  $D$  is the width of the actively radiating face. Focusing will narrow the field only in the near field region by reducing it to the width given by the beam divergence angle defined above. As a consequence the

minimum focused beamwidth at any range is given by:

$$\text{beamwidth} \approx \lambda R/D \quad (2)$$

where  $R$  is the range.

The directivity function gives the field amplitude relative to the peak pressure as a function of the off-axis angle  $\theta$  or distance,  $x$ . This function has the general form:

$$J_1[(\pi D/\lambda) \sin \theta]/[(\pi D/\lambda) \sin \theta] \quad (3)$$

For round, and

$$\sin(\pi D x/\lambda)/(\pi D x/\lambda) = \text{sinc}(D x/\lambda) \quad (4)$$

for rectangular apertures.  $J_1(x)$  is the first order Bessel function of the first kind (8).

Shading or apodizing the vibration amplitude across the face of the ceramic will minimize the secondary maxima predicted by Eqs. (3) and (4), and seen in Fig. 2. These equations express the fact that the field in the lateral direction in either the far field or the focal region of a transducer is given by the inverse Fourier transform of the excitation function, which facilitates selection of suitable apodization functions. Steinberg (9) has shown that for the rectangular aperture typical of an array element the highest sidelobe is only  $-13.4$  dB relative to the main beam, which results in a  $-26.8$  dB level for a pulse-echo system. A raised cosine apodization has a  $-64$  dB pulse-echo sidelobe level, which is acceptable for medical systems. The Gaussian apodization theoretically results in no sidelobes at all. The window functions used for apodization are realized by changing the area of the electrodes for single elements, or by changing the relative weight given to the signals to or from the elements of an array. This is discussed further in the next section.

The focusing used in medical transducers is often very weak. If the sagittal delay in the lens is less than a period at the center frequency we do not find the sharp focal spot seen in optics. Instead, the field has a more gradual relative maximum in the range direction at the focus (10). This weak focusing characteristic is useful in transmit where the beam must cover a certain depth in the range direction, as shown in Fig. 5(a). Weak focusing is also realized in the elevation direction of arrays with spherical lenses or element curvatures. The width of the focused field is at a minimum at the focal distance, and is given everywhere by Eq. (2).

The electrodes used for connection to the ceramics are vacuum deposited metals such as nickel or gold with provisions for connections to electrical coaxial cables. These connections are usually made by plating the electrode on the ceramic over to a holding or mounting structure to which wires can be soldered.

## ARRAYS

### Construction

An array consists of a number of individual single-element ceramics arranged to provide control of scanning and focusing functions by electronic means; see Fig. 4. They offer several advantages. The active aperture can be increased dynamically to keep  $D$ , Eq. (2), proportional to range,  $R$ . This is called

an expanding aperture design. Dynamic or time-adjusted focusing can be applied as well. The result is to maintain a nearly constant and small resolution element throughout the images. Synthetic aperture processing can also be used with arrays. The electronically scanned arrays have no moving parts which increases their reliability.

Arrays are usually constructed by cutting the elements from a larger piece of ceramic or composite material. The small element area and number of connections introduces some additional complications in construction and operation from those seen in the larger single-element transducers.

The individual array elements are mounted next to others, and waves excited in the lateral direction in the various materials can couple signals into other elements. This coupling is minimized by running the dicing cuts all or part way through the sandwich, which may include the backing and matching layers as well as the ceramic. The small array elements need to be supported during manufacture. This is done by arranging the order in which the layers are applied, shaped by grinding or lapping and the necessary cuts made so that the dimensions of the whole assembly are maintained.

The individual array elements have a higher impedance than typical single element transducers so the electrical coupling must be optimized for this condition. The connections require many more cables which must be individually soldered to the electrodes, or attached by directionally conductive pads (11).

Many current generation ultrasound imaging arrays feature a fixed cylindrical focal element to focus the beam in the elevation direction and are often referred to as one-dimensional (1-D) arrays. More recent publications describing different array designs distinguish between 1.25-D and 1.5-D array structures which, in comparison with a 1-D array, offer improved focal depth and image resolution. A 1.25-D array is a multirow array with variable elevation aperture controlled as a function of time after transmit by switches. The 1.5-D arrays further extend the 1.25-D array properties by providing connections that may be used for dynamically adjusting the elevation aperture, apodization, and focus; see Fig. 7.

## DESIGN

The design process starts with considering the medical application to specify the areas to be imaged and the image planes

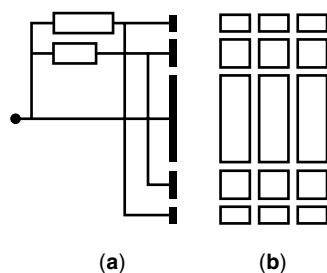


**Figure 7.** Construction of arrays with controllable elevation angle or slice width: (a) connections to an array element that is subdivided into sections in the vertical direction; (b) frontal view of elements of such an array. For a 1.25-D array the boxes in (a) contain switches for expanding the aperture with range. In a 1.5-D array the boxes contain variable delays for focusing and variable gains for apodization.

**Table 2. Sources of Design Software**

*PZFlex; Weidlinger Associates*

375 Hudson Street  
New York, NY 10014-3656  
(212) 367-3000

or:

4410 El Camino Real  
Suite 110  
Los Altos, CA 94022  
(415) 949-3010  
<http://www.weidlinger.com>

*ANSYS; Ansys, Inc.*

Southpointe  
275 Technology Drive  
Canonsburg, PA 15317  
(412) 746-3304  
<http://www.ansys.com>

*PiezoCAD; George Keilman*

Sonic Concepts  
20018 163rd Ave. NE, Woodinville, WA 98072  
(425) 485-2564/7446  
75227.3361@compuserve.com

*FIELD, by Jørgen A. Jensen*

Dansk Technical University  
download information and program from:  
<http://www.it.dtu.dk/~jaj/field/field.html>

*PSpice™; Microsim Corporation*

20 Fairbanks, Suite 198  
Irvine, CA 92718  
(714) 770-3022  
<http://www.microsim.com/>

desired. In medical applications the anatomy and attenuation of tissue set the size of the imaging window and frequency of operation. The frequency imposes a tradeoff between depth of penetration and the achievable resolution (1) The type of transducer (single element, array, etc.) is considered to achieve acceptable spatial and temporal resolution at a given frame rate. Then the process continues with acoustic beam design and the array architectures to achieve it. Selection of appropriate piezoelectric and other materials and of construction details follows. The materials and construction methods chosen have a major impact on cost of production since the imaging transducer is probably the most expensive single component in an imaging system. Some available computer tools for imaging transducer design are given in Table 2.

All designs must be assessed for safety on the basis of Food and Drug Administration (FDA) guidelines (12). Both tissue heating and mechanical cavitation are possible. The initial designs can estimate the acoustic intensities in tissue using the tools listed in Table 2, but measurements with calibrated probes are needed for FDA certification.

The electrical design then follows to provide for the needed transmitter output power as well as damping and good signal-to-noise ratio on receive. As is usual in design, these steps

may be iterated several times. There is no single method or approach that handles all of these aspects of design, and extensions to wideband pulse operation are not complete for some of them. Continuous wave theory, as in Eqs. (1) to (4), is useful for initial approximations, and can be used with Fourier methods for time-domain calculations. Design methods are under continuous development at present. Construction details of commercially available transducers are considered proprietary information, so little explicit illustration is possible.

### Acoustic Beam Design

The design of single element transducers and individual array elements to produce a desired acoustic field can be started using the Fourier relationship mentioned previously to relate the resolution to the transducer aperture. The design of the full array is similar to that for radar. The theory for radar arrays has advanced to the point of synthesis, but for medical ultrasound important differences complicate the picture. Field synthesis in radar is possible because these arrays are concerned with narrowband fields at a great distance. In practice the analysis concerns the field shapes at infinity. However, in medical applications the image is desired to be produced starting from the transducer surface. In addition, although medical ultrasonic arrays could be synthesized (at least at the focal region) by using the same methods as in radar, there are many differences that require careful consideration.

These differences can be explained by considering Fig. 8, which illustrates beam formation by the two types of linear array. The radiated field in both cases is the product of two factors, the directivity function of the whole aperture, called the array factor, and the directivity functions of an individual element. Both can be approximated by Eqs. (3) and (4) using the appropriate value for  $D$ .

The array factor in medical imaging is the directivity function of that part of the array which is excited (or connected) at any given time. It consists of a main lobe, as given in Eq.

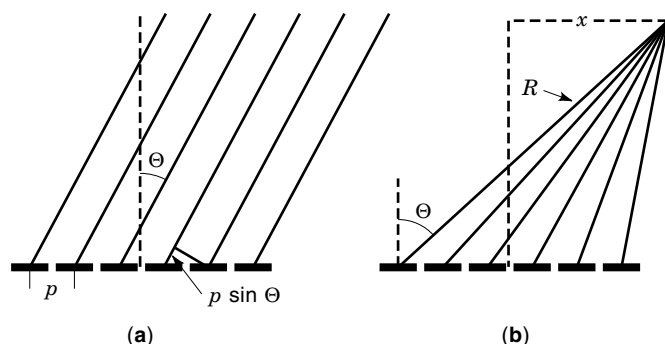


**Figure 8.** Comparison of scanning arrays. Plan view of the beam scanning typical of a radar array is shown at (a), where a beam is formed in every direction the array pitch,  $p$ , and off-axis angle  $\Theta$  satisfy the condition that  $p \sin \Theta$  is one wavelength. At large scan angles there may be more than one value of  $\Theta$  that satisfies this condition. At this angle a grating lobe will exist that is equally as strong as the desired lobe. In a typical ultrasound array with focusing in the near field, (b), the delays needed for beam steering at each element are calculated from the range,  $R$ , and are all different. Grating lobe formation is no longer simple since the angles  $\Theta$  also vary.

(1) and has additional lobes, called grating lobes in every direction in which the fields can add, as in a radar array; see Fig. 8(a). In between the main and the grating lobes are the sidelobes in the array directivity function. These added relative maxima in the field pattern can, theoretically, be in the imaged plane or behind the array. During scanning these grating and sidelobes can swing around from the reverse direction into the physical space (tissue) and generate false signals (often referred to as ghost images) from structures in directions other than that of the main beam. The grating lobes are at  $\theta = \pm 90^\circ$  for one wavelength spacing of the array elements, and there is one at  $180^\circ$  for half-wave spacing. The main beam will also change shape from the change in the projected area of the elements, and from the array factor.

The element directivity functions just given were for rectangular elements. Equation (1) applies to each element, with  $D$  being the width in the scan plane for finding image resolution, or in the vertical dimension of the element for calculating the elevational or out-of-plane beam width. Elements with a narrow directivity function in azimuth may be used to reduce the array side and grating lobe levels, as in radar, but such directivity will reduce the number of elements that can contribute to the main beam, particularly when scanning off-axis. This is a major problem since the scan angles needed in medical arrays,  $\pm 45^\circ$ , for example, are much larger than those needed in radar.

The time delays needed to focus the elements in the near field are not simple multiples of each other as in scanning radar, as can be seen from Fig. 8(b). The needed delays calculated from an illustration like Fig. 8(b), usually are stored in memory, and used to control the beamformers. Since the off-axis angles of the individual beams are not the same for all elements, the optimization of transducer design in order to minimize the amplitude of grating and sidelobes is much more complicated. Generally, the element spacing must be set at slightly less than the wavelength limit.

Apodization of the array can be used to reduce the array factor sidelobes (but does not affect the grating lobes) and is accomplished by varying the drive voltage or the receiver gains on the different elements. Another strategy for reducing grating lobes is to connect different sets of array elements to the transmitter than those used for receiving. The grating lobes for each pattern then can be set not to be in the same direction.

Calculation of the field that results from apodization, delaying and switching of a truly wideband transmitted pulse is quite complicated, but has been made easier using computer programs. The basic difference between the radar and ultrasound imaging array calculations is that, in ultrasound, the field amplitudes and beam shapes are found by scalar addition of the pressure waves from the excited elements, rather than using vector field addition as in radar.

Most texts present the field calculations for continuous waves, using the Huygens principle or the Rayleigh integral (13) There are some remaining theoretical problems with this approach, besides the complication of converting the result into the time domain (14) An alternative to the continuous wave solutions in current texts is to use the spatial impulse response to calculate the field generated by the array architecture under consideration (15) This is an inherently wideband, time-domain method. The overall system function is found by convolving together the transmitter impulse re-

response with the electrical transmitter waveform and the impulse response calculated from the receiving beam.

One available program, FIELD, see Table 2, uses the impulse response method to calculate the fields from linear arrays with specified apodization, expanding apertures, dynamic focusing, and beam steering. It also can create the signal received from this or a different element choice, so that images can be produced from specified targets. Files of digital computer phantoms are provided as well, so the images that result from a trial array and beamformer design can be calculated.

### Finite Element Models

A combination of three-dimensional materials design and acoustic field calculation is possible using a finite element modeling (FEM) program. These can give guidance in acoustical design of composite materials as well as in assessing array performance, including the dicing pattern, interelement coupling, apodization, and the lens (16) Since computers are becoming faster every year this method is becoming increasingly useful. Two major programs are available commercially, ANSYS and PiezoFLEX. See Table 2 for sources. They are particularly useful for investigating lateral modes in ceramics and interelement coupling in arrays. Animations of motions, such as flexural vibrations of ceramic pillars, is particularly useful to correct problems caused by spurious resonances.

Modeling of composite materials requires a very fine analysis mesh since the ceramic bodies in composites are much smaller than a wavelength. In contrast, other areas such as the backing are relatively large, so provision for multiscale modeling is helpful. These programs can change methods to calculate the radiation pattern using the Rayleigh integral, and substitute a boundary condition for the backing. The main drawback in FEM modeling is the need to determine accurate material properties. The shear wave properties are particularly difficult to measure accurately, and the materials may change their properties during the bonding and grinding operations of assembly.

### Circuit Models

The basic equations needed to analyze piezoelectric transducers in the frequency domain are found by combining those of piezoelectricity, elasticity, and one-dimensional wave propagation into one common matrix. This matrix, Eq. (5), treats the vibrating element as a three-port with forces, velocities, voltages and currents at the ports as either boundary conditions or variables.

$$\begin{pmatrix} F_1 \\ F_2 \\ V_3 \end{pmatrix} = -j \begin{pmatrix} Z \cot \beta l & Z \operatorname{cosec} \beta l & h/\omega \\ Z \operatorname{cosec} \beta l & Z \cot \beta l & h/\omega \\ h/\omega & h/\omega & 1/\omega C_0 \end{pmatrix} \begin{pmatrix} V_1 \\ V_2 \\ I_3 \end{pmatrix} \quad (5)$$

Here the  $F$ 's are the forces and the  $V$ 's are the inward directed velocities at the front and back faces of the transducer.  $V$  and  $I$  are the voltage at and the current into the electrical port. The mechanical impedance,  $Z$ , is the characteristic impedance of the ceramic times the radiating area,  $C_0$  is the capacitance of the element, and  $h$  the piezoelectric constant. The variable  $\beta l = \pi \omega / \omega_0$ , where  $\omega$  is the angular frequency and  $\omega_0$  the half-wave resonance. This treatment is restricted to one-dimen-

sional wave propagation, that is, elements that are many wavelengths in diameter, or that are mounted in an array with a number of adjacent radiating elements.

Although these equations and the boundary conditions that determine the relations between the variables at the acoustic terminals can be solved directly to analyze the behavior of a mounted single element transducer, either alone or in an array, many engineers have found it instructive to use an electromechanical analogy to derive an equivalent circuit, followed by writing out loop and node equations for calculations. Using the equations or equivalent circuits ignores factors due to lateral waves, and cannot give spatial or beam information if used alone. The Mason and KLM equivalent circuit models are equivalent; both satisfy these equations and provide suggestions for the initial transducer design. Commercial software is available for their use.

### Mason Model

The circuit derived by Mason as modified by Redwood is shown in Fig. 9(a). It is convenient for analyzing transducer operation with short pulses and visualizing reflections at the faces. Transmission lines and resistances can be attached to the faces to represent the matching and backing layers.

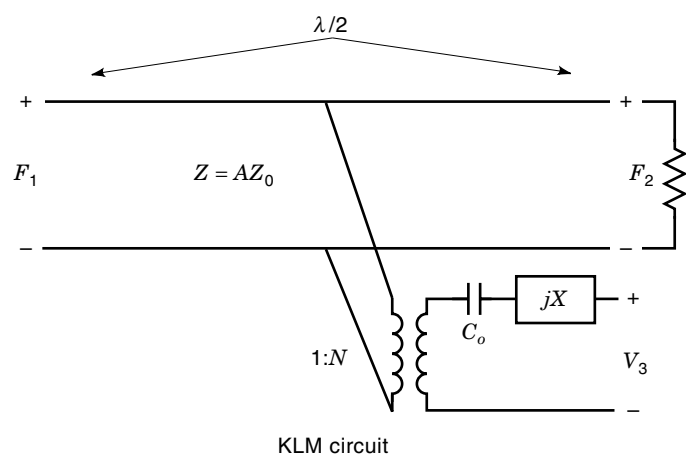
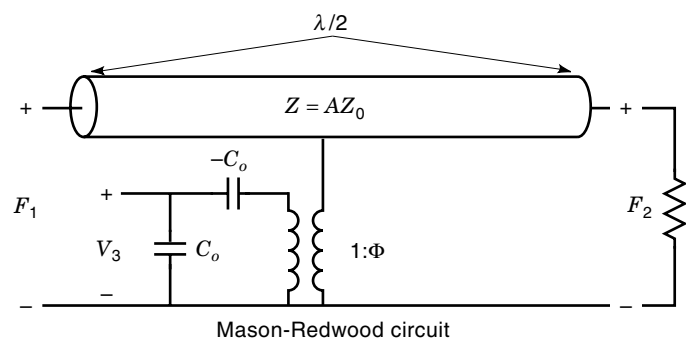


**Figure 9.** Circuits that are equivalent to Eq. (5), using the force-voltage analogy. The resistances illustrate the connection to external loads.

$Z_0$  = acoustic impedance of ceramic,  $C_0 = \epsilon A/l$ ;  $A$  is the radiating area;  $l = \lambda/2$ , and  $\Phi = hC_0$ .  
 $N = k_z(\pi/\omega_0 C_0 Z_0)^{1/2} \operatorname{sinc}(\omega/2\omega_0)$   
 $X = (k_z^2/\omega C_0) \operatorname{sinc}(\omega/\omega_0)$

This model has been implemented on the widely available circuit analysis programs, Spice and PSpice, see Table 2, so that pulse operation in the time domain can be analyzed as well as frequency domain analysis of matching circuits (17). A major advantage of this approach is that these programs can include the actual transmitter and receiver circuits being considered, since semiconductor models are in the Spice libraries. This is important since modern systems use many different transducers with the same transmitter and receiver. Design must often be analyzed in either of two ways, to find the optimum transmitter and receiver initially, or to optimize the transducer design for fixed electronics.

The Mason-Redwood model has recently been adapted for use with the FIELD program to provide a more complete simulation model for system analysis and calculations of radiated power (18).

#### KLM Model

Another model, called the KLM after its originators, is convenient for writing circuit equations since only a single loop is needed for each port; see Fig. 9(b). Again, backing and matching layers can be included in the model. Commercial software, PiezoCAD, is available for this model; see Table 2. Values of the electrical resistances of the transmitter and receiver have been used with this program to optimize designs, including transmitter efficiency and receiving signal-to-noise ratio (19).

#### Electrical Design

Matching and damping can be assessed by using the Spice models alluded to in the last section, but there are a number of strategies to consider. Transmitter matching is relatively unimportant in many designs since the average electrical transmitter power level is low and power transfer is seldom an issue unless the output stages are mounted in the probe. Damping by the receiver is much more important, since it can help the energy stored in the vibrating element to ring down so the receiver can recover from overload by the transmitter in time to amplify echoes from nearby structures. The matching to the receiver amplifier must also consider the signal-to-noise ratio to allow weak signals from greater depths in tissue to be seen. Unfortunately, the ceramics with a high electroacoustic coupling coefficient have a high capacitance which restricts the electrical bandwidth unless the receiver input impedance level is kept quite low. Some equalization in the probe or later in the receiver could compensate for the effects of this capacitive loading. The loading can come from the connecting cables as well as from the ceramic element.

At the half-wave resonance frequency the electrical impedance of a piezoelectric transducer is represented by a parallel  $R$ - $C$  circuit. The impedance presented to the transmitter or receiver can be made a low resistance if a simple tuning inductor is connected in series with the transducer, or a higher impedance if it is connected in parallel, to tune out the capacitive reactance. More complex matching elements may be included in the probe housing or connector, or implemented in software. Oakley (19) has shown that simple low impedance loading of the transducer can make the receiver signal-to-noise ratio (SNR) independent of the capacitance of the ceramic over a wide range of values.

## CURRENT DEVELOPMENTS

### Construction

The construction methods and materials used are highly proprietary. The major manufacturers maintain their own databases of material properties. This is a rapidly changing area with the latest information from materials research being presented at technical meetings. Selfridge (20) has published some materials data and others are in standard references (21).

In multilayer designs several thin layers of ceramic or composite can be stacked in the thickness dimension to form an equivalent vibrating element. If the electrodes are connected in parallel this multilayer construction can reduce the high impedance of 2-D array elements to acceptable levels (22). This approach has the added complication of requiring connections to be made through the half-wave thickness of the material.

The multilayer approach also can yield a wideband nonresonant design if the layers are made unequal in thickness (23). The highest frequency is set by the thickness of the thinnest layers.

### 2-D Arrays

Arrays with the radiating elements diced fully in two dimensions and connected separately to the electronic circuits offer the possibility of doing true three-dimensional imaging. The beam can be directed with full electronic apodization, focusing, and steering to a region that is as small in elevation as in azimuth. This is important since the whole volume of the pulse packet will produce clutter signals, as in radar, which degrade the image contrast if there are any scatterers close to the target. Annular arrays offer the same benefits but require mechanical scanning. A proposed intermediate array type called a 1.75-D array has more elements in elevation than the 1.5-D array, but less than the 2-D. They can steer the beam over a limited range in elevation.

This 2-D construction introduces additional problems that are currently being attacked. First, the impedance of each small area element is quite high, requiring high transmit voltages and making the cable capacitance more important in limiting the bandwidth on receive. At the same time the number of connections required has led to innovative connection methods, using materials that are conductive in only one direction as a sandwich between the array connection pads and a cable terminating structure. The large number of separate coaxial conductors also makes the connecting cable rather stiff and awkward to handle, which is a problem for the operators even with present linear arrays.

Recently, a successful implementation of an experimental 2.5 MHz two-dimensional  $50 \times 50$  element phased array has been reported. The implementation required the use of an innovative electrically conducting anisotropic elastomeric backing. The active aperture of the array was limited to 15 mm to comply with the typical acoustic window between the ribs for transthoracic examinations. The elements were spaced at  $\lambda/2$  to provide full steering and focusing capability without grating lobes (111).

There are two approaches suggested to simplify 2-D array construction. The approach used in radar of using sparse arrays can be used. This is done by eliminating elements, ac-



ording to some plan, either deterministic or random, to obtain an acceptable image resolution and grating lobe level with fewer array elements than in a fully filled array. Another is to mount the beamforming electronics in the probe. There can be enough area under each piezoelectric element to consider integrating these circuits there, so that only a few cable connections are needed.

### Design

The design methods presented to date are primarily for analysis of a given, and simple, structure rather than for synthesis. The initial designs, for example, use regular structures for the pillars in composites and the spacing of the elements in an array. These regular structures can support strong spurious vibrations that must be avoided. The only other design plan that can be handled analytically at present is the fully random structure that has been used in radar arrays. It is an open question whether a deterministic pattern exists that would be optimum (or even better) for use. These could lead to more economical thinned arrays and perhaps to better composite materials.

### BIBLIOGRAPHY

1. L. A. Frizzell and K. Thomenius, Ultrasonic Medical Imaging, in J. G. Webster (ed.), *Encyclopedia of Electrical and Electronics Engineering*, New York: Wiley, 1999.
2. D. A. Berlincourt, D. R. Curran, and H. Jaffe, Piezoelectric and piezomagnetic materials and their function in transducers, in W. P. Mason and R. N. Thurston (eds.), *Physical Acoustics: Principles and Methods, Vol I A*, New York: Academic Press, 1979.
3. R. A. Lemons and C. F. Quate, Acoustic Microscopy, in W. P. Mason and R. N. Thurston, (eds.), *Physical Acoustics: Principles and Methods, Vol XIV*, New York: Academic Press, 1979, pp. 1–92.
4. L. W. Kessler and D. E. Yuhas, Acoustic microscopy—1979, *Proc. IEEE*, **67**: 526–536, 1979.
5. W. A. Smith and B. A. Auld, Modelling 1-3 Composite piezoelectrics: thickness-mode oscillations, *IEEE Trans. Ultrason. Ferroelectr. Freq. Control*, **38**: 40–47, 1991.
6. W. A. Smith, A. A. Shaulov, and B. A. Auld, Design of piezocomposites for ultrasonic transducers, *Ferroelectrics*, **91**: 155–162, 1989.
7. C. S. Desilets, J. D. Fraser, and G. S. Kino, The design of efficient broad-band piezoelectric transducers, *IEEE Trans. Sonics. Ultrason.*, **25**: 115–125, 1978.
8. B. D. Steinberg, *Principles of Aperture and Array System Design, Including Random and Adaptive Arrays*, New York: Wiley, 1976.
9. Ref. 8, Chap. 4.
10. G. S. Kino, *Acoustic Waves: Devices, Imaging and Analog Signal Processing*, Englewood Cliffs, NJ: Prentice-Hall, 1987, 191–194.
11. M. Greenstein et al., A 2.5 MHz 2-D array with Z-axis electrically conductive backing, *IEEE Trans. Ultrason. Ferroelectr. Freq. Control*, **44**: 970–977, 1997.
12. Information for manufacturers seeking marketing clearance of diagnostic imaging systems and transducers, Document issued September 30, 1997 by U.S. Dept. of Health and Human Services, Food and Drug Admin., Center for Devices and Radiological Health, Rockville, MD.
13. Ref. 10, pp. 158–163.
14. J. M. Reid, The Measurement of Scattering, in J. F. Greenleaf (ed.), *Tissue Characterization with Ultrasound*, Boca Raton FL: CRC Press, 1986, pp. 105–108.
15. J. A. Jensen and N. B. Svendsen, Calculation of pressure fields from arbitrarily shaped, apodized, and excited ultrasound transducers, *IEEE Trans. Ultrason. Ferroelectr. Freq. Control*, **39**: 262–267, 1992.
16. N. N. Abboud et al., Finite element modeling for ultrasonic transducers, Ultrasonic Transducer Engineering Conference, K. Shung (ed), in *Proc. SPIE Symp. Med. Imaging*, Bellingham, WA: SPIE, 1998.
17. A. Puttmer et al., SPICE model for lossy piezoceramic transducers, *IEEE Trans. Ultrason. Ferroelectr. Freq. Control*, **44**: 60–65, 1997.
18. E. Maioue et al., *PSPICE modelling of ultrasound transducers: Comparison of software models to experiment*. Submitted for publication.
19. C. G. Oakley, The calculation of ultrasonic transducer signal-to-noise ratios using the KLM model, *IEEE Trans. Ultrason. Ferroelectr. Freq. Control*, **44**: 1018–1026, 1997.
20. A. R. Selfridge, Approximate material properties in isotropic materials, *IEEE Trans. Sonics Ultrason.*, **32**: 381–394, 1985.
21. Ref. 4, Appendix B.
22. R. L. Goldberg et al., Modeling of piezoelectric multilayer ceramics using finite element analysis, *IEEE Trans. Ultrason. Ferroelectr. Freq. Control*, **44**: 1204–1214, 1997.
23. Q. Zhang, P. A. Lewin, and P. E. Bloomfield, PVDF transducers—a performance comparison of single-layer and multilayer structures, *IEEE Trans. Ultrason. Ferroelectr. Freq. Control*, **44**: 1148–1155, 1997.

JOHN M. REID  
PETER A. LEWIN  
Drexel University

**ULTRASOUND FLOW MEASUREMENT, MEDICAL.** See FLOW TECHNIQUES, MEDICAL.  
**ULTRASOUND, HIGH POWER.** See HIGH POWER ULTRASOUND.  
**ULTRASOUND, MEASUREMENT OF.** See DOSIMETRY.